14th Australasian Fluid Mechanics Conference
Adelaide University, Adelaide, Australia
10-14 December 2001

Preliminary Study of Oscillating Triangular Jets

S. K. Lee, P. V. Lanspeary, G. J. Nathan, R. M. Kelso and J. Mi

Department of Mechanical Engineering
Adelaide University, Adelaide, South Australia, 5005, AUSTRALIA

Abstract

A visualisation experiment and measurements with a Pitot probe show that fluidic instability of a partially confined triangular jet can produce a continuously oscillating flow. The device which produces this flow consists of a triangular inlet orifice expanding into a short axisymmetric chamber with an exit lip. These oscillations occur over a wide range of chamber lengths and expansion ratios. The amplitude of oscillation and the initial spreading angle of the jet flow are much larger than that of a simple jet flow. The external oscillating jet has preferred azimuthal directions which are aligned with the corners of the triangular orifice. The energy loss coefficient of these jets is significantly lower than what can be achieved from a precessing circular jet.

Introduction

Oscillating-jet flows can produce turbulence very different from the fully developed turbulence of simple jets. Very large velocity fluctuations produced by oscillating jets are the source of large scale turbulent mixing [8,16], large spreading angles [6,10], large initial decay rates of mean velocity [1,3] and high rates of mass entrainment from the surroundings. Mechanical devices [14,15] can drive large-scale oscillations of the bulk flow but they require high levels of maintenance and have limited durability in harsh industrial environments. In contrast, acoustic devices excite the growth of regular oscillations within the jet shear layers [9,12] but they are also very noisy.

Devices such as the fluidic precessing jet (FPJ) use aerodynamic instability to produce large-scale oscillations in the flow. They present fewer practical difficulties than mechanically or acoustically driven devices and they operate successfully in high-temperature environments such as cement [11], alumina, zinc oxide and lime [2] kilns. The success of the FPJ has encouraged interest in other ways of producing fluidically excited flows [4].

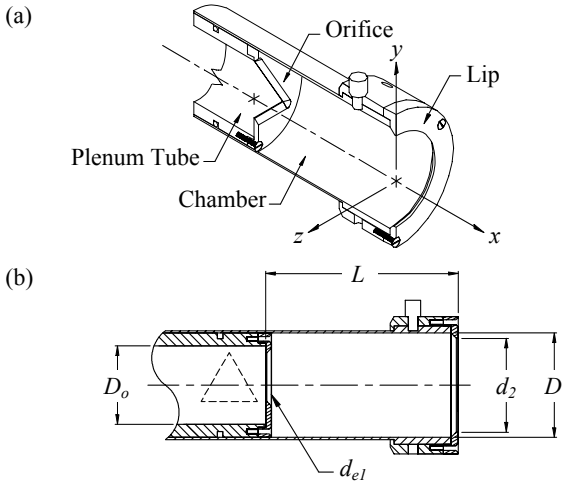

Figure 1. Oscillating jet nozzle (a) components and (b) parameter definitions.

There is particular interest in devices which produce oscillating jet flows, are compact, produce low pressure loss and have no moving parts.

Oscillating Jet Nozzle

Figure 1 describes the geometry of a device that produces an oscillating jet. The device consists of a chamber with a fixed internal diameter $D = 54.75$ mm and a length L which is adjustable within the range $0 \le L/D \le 5.5$. Triangular orifices of various sizes can be installed at the inlet end of the chamber. The orifices are equilateral and have a 45° chamfer to ensure that the flow separates at the upstream face. The size of the orifice is defined in terms of the "equivalent" diameter, d_{el}, of a circle with the same area. Four triangular orifices (*E1*, *E2*, *E3* and *E4*) and a circular orifice (*CO*) were manufactured for this investigation. The sizes, contraction ratios (D_o/d_{e1}) and expansion ratios (D/d_{e1}) of these orifices are given in Table 1.

With the circular orifice inlet (*CO*), which has the same expansion ratio ($D/d_{e1} = 5$) as industrial precessing-jet nozzles, it is possible to compare the flow from the FPJ nozzle [6] with the flow from the oscillating-jet nozzle (triangular orifice). For both oscillating-jet and FPJ nozzles, the diameter of the lip at the exit plane is $d_2 = 0.9D$.

Experimental Apparatus

The air supply for the oscillating-jet nozzle is taken from a 200cfm (340 m^3/h), 700kPa industrial air compressor and is regulated to 210kPa in the laboratory. The flow rate is measured with a Fischer & Porter (FP-3/4-27-G-10) flow-meter tube and a wide selection of floats.

The oscillating jet nozzle is attached to a straight tube of internal diameter $D_o = 41.2$ mm and a length equal to 50 diameters. At the inlet end of the tube, a "honeycomb" of plastic drinking straws ($l/d = 12$) removes any residual swirl and a wire-mesh screen with an open area ratio of 60% improves the uniformity of the flow. This flow conditioning produces an axisymmetric fully developed turbulent pipe flow immediately upstream from the inlet orifice of the oscillating jet nozzle. The horizontal axis of the jet flow is approximately halfway between the floor and the ceiling of the laboratory. To reduce the effect of draughts, the jet flow is enclosed on three sides by a rectangular (2.0 m × 2.0 m × 3.5 m long) cage made of woven fibreglass screen. The downstream end of the screen cage is open.

Nozzle	Orifice Shape	D_o/d_{el}	D/d_{el}	d_{el} (mm)
E1	Equilateral Triangle	1.58	2.10	26.07
E2		1.88	2.50	21.90
E3		2.26	3.00	18.25
E4		2.63	3.50	15.64
CO	Circle	3.76	5.00	10.95

Table 1. Geometries of the oscillating-jet nozzles.

Jet Spreading Angle

Initial evidence of jet oscillation was obtained by anchoring a silk-ribbon streamer at the centre of the nozzle exit plane and then observing the motion of the streamer in the jet flow. The amplitude of oscillation can be estimated from side-view photographs of the streamer. Time averaging is performed by exposing each film image for 5 to 10 seconds. The time-averaged images in Figure 2 are typical of those obtained in these experiments. Maximum visible included spreading angles of the streamer, θ, from the photographs are plotted in Figure 3 as functions of chamber length. These tests were run at an orifice Reynolds number of $\mathrm{Re}_1 = d_{e1}U_1/\nu = 50{,}000$.

For very short chamber lengths ($L/D < 1$), the behaviour of the emerging jet is indistinguishable from that of a simple jet. As the chamber length increases, the spreading angle of the streamer begins to increase without large-scale oscillation. For the two largest expansion ratios (*E3* and *E4*), the increased spreading angle is accompanied by an increasing asymmetric deflection towards the wall of the chamber. The azimuthal angle of the deflection is fixed. Fixed azimuthal deflection occurs over only a very small range of L/D ratios. As this range is exceeded, the streamer deflection develops into large-scale oscillations. For the two smallest expansion ratios (*E1* and *E2*), the transition from simple jet to oscillating jet appears to be direct, that is, without any intermediate fixed deflection. In the available data, there is no apparent step increase in streamer spreading angle at the transition to oscillating jet.

With the triangular orifices, oscillation or asymmetric transition begins in the range $1 < L/D < 1.25$. The oscillations are continuous. The growth rate of the spreading angle increases as the expansion ratio D/d_{e1} of the orifice increases. The maximum spreading angle and the L/D ratio which produces it are also increasing functions of D/d_{e1}.

For the circular orifice, oscillations occur within a much narrower range of chamber lengths, $2.3 < L/D < 2.8$, and the oscillations themselves are intermittent (in time) rather than continuous. The maximum included spreading angle of about 170° is much larger than that observed for the triangular orifices. Nathan *et al*. [6] identify this as the fluidic precessing jet flow.

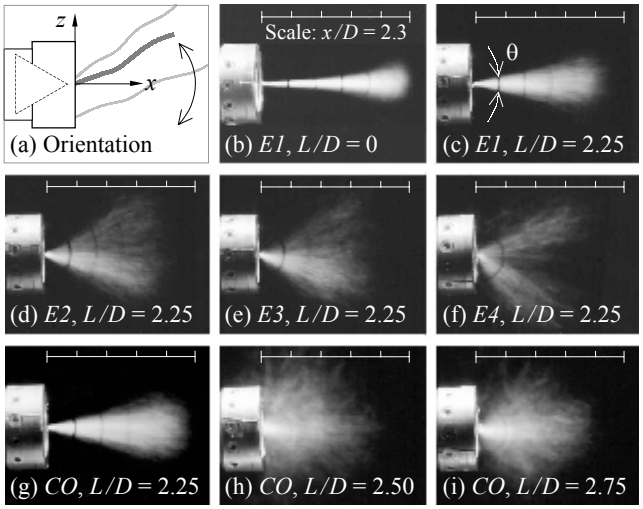

Figure 2. Flow visualisation of oscillating-jets: (a) nozzle orientation; (b)-(f), triangular orifice; (g)-(i), circular orifice. Each image is time average over 5 seconds. $\mathrm{Re}_1 = 50{,}000$.

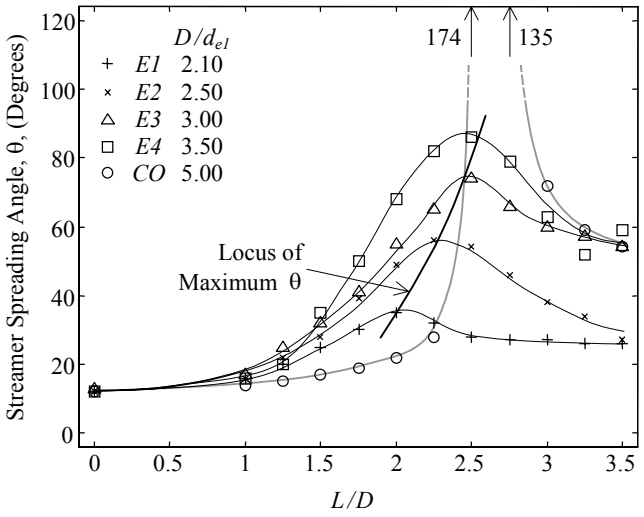

Figure 3. Initial streamer spreading angle, θ, measured from the side-view photographs. +, ×, Δ, □, triangular orifice; ○, circular orifice. $\mathrm{Re}_1 = 50{,}000$.

As the chamber length increases beyond 2.8*D*, the spreading angle and the precession of the circular jet collapse to a "long-cavity mode" [5]. The long-cavity jet fills the outlet plane of the nozzle and has no easily identifiable characteristic frequency. The data suggest that the oscillating jet from a triangular orifice collapses to a similar long-cavity mode as L/D increases beyond the value which produces maximum spreading angle.

Preferred Azimuthal Direction

Observation from downstream of the nozzle reveals that the oscillating triangular jet has preferred azimuthal directions. Figure 4 is a short sequence of 3 images from a series of 270 photographs. The time interval between photographs is 0.25 seconds and the streamer is illuminated from above. From each of these images it is possible to estimate ϕ, the azimuthal angle of the streamer. Inspection of the images suggests that ϕ is not a uniformly distributed function of time. The distribution of ϕ is estimated by dividing each image into a "clock face" of 12 azimuthal segments and counting the streamer direction in each image into one of four adjacent segments. The result, obtained from 1080 images, is a polar plot (Figure 5(b)) of the probability density, $p(\phi)$. Figure 5(b) indicates that the external oscillating jet has preferred directions aligned with the corners of the triangular orifice.

The preferred directions of alignment are a result of azimuthal variation in the length scale of velocity fluctuations immediately downstream from the triangular orifice. Length scales midway between the corners are much larger than length scales near the

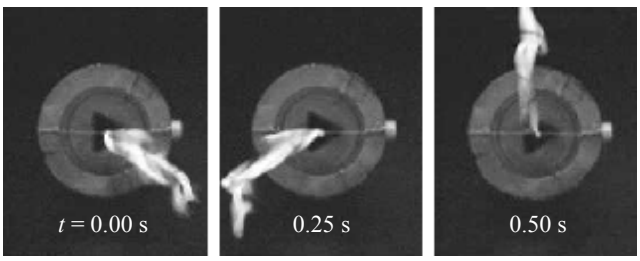

Figure 4. Sequence of photographs showing oscillation of a silk-ribbon anchored at the centre of the exit plane. The camera is far downstream of the nozzle, which has orifice *E3* and $L/D = 2.5$. The time between images is 0.25 seconds. $\mathrm{Re}_1 = 50{,}000$.

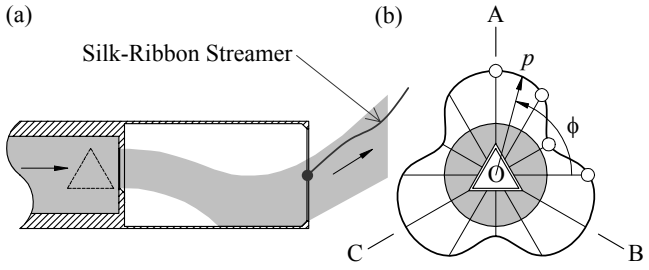

Figure 5. Preferred azimuthal orientation of the emerging jet:
(a) Simplified diagram of the emerging jet in one of the preferred azimuthal alignments OA, OB or OC.
(b) Estimated probability density, $p(\phi)$, of the azimuthal directions of the streamer. Data is shown as circles. $p(\phi)$ is assumed to have three-fold axial symmetry.

corners [13], and so the largest entrainment rates, mixing rates, and jet-spreading rates also occur midway between the corners [7]. The jet from the orifice is therefore expected to attach to the chamber wall at preferred azimuthal angles which are midway between corners. The asymmetric jet emerging from the nozzle would then be deflected by the lip so that it passes across the face of the exit. This is the jet alignment shown in Figure 5(a).

Velocity Decay Rate

In the self-similar region of a turbulent jet, the reciprocal of the centreline velocity and the width of the jet are proportional to the distance from the virtual origin. The product of centreline velocity and width is constant. The mean slope, Λ, in the linear region of $U_{\max\text{-}cl}/U_{cl}$ versus x/d_{e1} curve is therefore a convenient measure of jet spreading rate.

Figure 6 shows, for each of the oscillating-jet nozzles, the variation in Λ as a function of L/D. The velocity measurements were obtained from a Pitot probe and a Baratron pressure transducer. For each velocity measurement, the transducer output was averaged for 3 to 5 minutes on a digital oscilloscope, and each value of Λ was determined by linear regression from 4 or 5 velocity measurements. The smallest correlation coefficient of linear regression for orifice *E4* was 0.994; for the other orifices, the correlation coefficients were larger than 0.999.

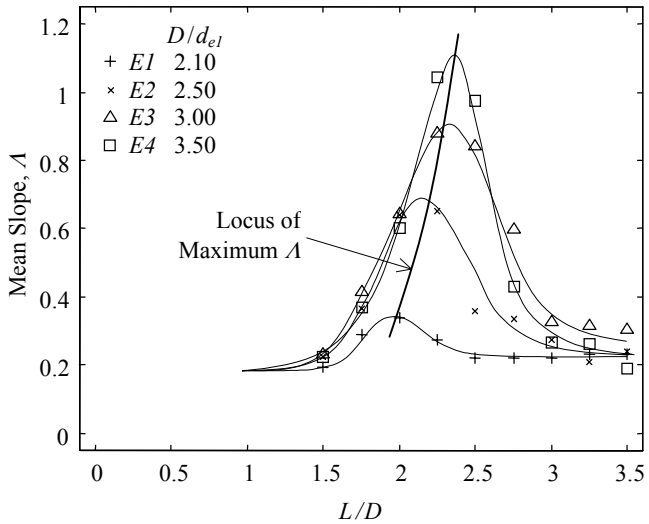

Figure 6. Mean slope, Λ, determined from the linear region of $U_{\max\text{-}cl}/U_{cl}$ versus x/d_{e1} data. +, ×, Δ, □, triangular orifice. $\mathrm{Re}_1 = 50{,}000$.

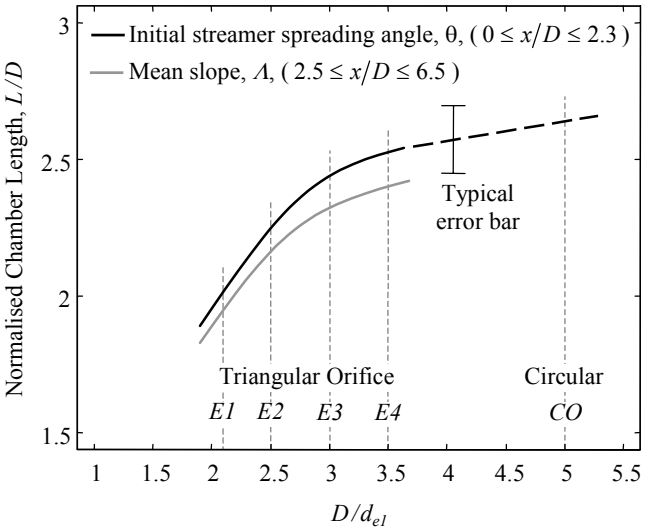

Figure 7. Domain of maximum streamer spreading angle, θ, and mean slope, Λ, for $\mathrm{Re}_1 = 50{,}000$.

The measurements for Figure 6 were obtained at distances of 2.5 to 6.5 chamber diameters from the nozzle. Near-field induced flow-reversal has a negligible effect on the velocity measurements if the Pitot probe is further than 2.5*D* from the nozzle exit plane. At distances $x/D > 6.5$, the signal to noise ratio is unacceptably low.

The rate of velocity decay in an FPJ is much greater than in the oscillating jet from a triangular orifice. The decay rate is so large that, even for a flow velocity of about 70 m/s at the orifice, Λ could not be measured with the available instrumentation.

In Figure 7, the L/D ratios required to achieve maximum spreading angle, θ, and maximum mean slope, Λ, are plotted as functions of the expansion ratio, D/d_{e1}. This indicates the chamber length required for maximum entrainment or mixing rate. These functions are in approximate agreement. The differences may be due to variation in spreading angle with distance from the exit lip or due to differences between the streamer spreading angle and the actual jet spreading angle.

Energy Loss Coefficient

The energy loss coefficient determines the relationship between pressure in the supply pipe and momentum of the jet flow at the exit lip. This affects the cost of the nozzle and of ancillary equipment such as compressors and fans. The loss coefficients, *K*, in Figure 8 were calculated from wall pressure, P_o, measured 10 pipe diameters upstream from the orifice, the pipe cross-section area, A_o, and the flow rate, *Q*:

$$K = \frac{P_o}{0.5\rho\left(Q/A_o\right)^2} + 1 \,. \qquad (1)$$

The important feature of Figure 8 is that the loss coefficients of the triangular orifice nozzles are much lower than the loss coefficient of the FPJ nozzle. This reduction is due primarily to the lower expansion ratios, D/d_{e1}, of the triangular nozzles. However, the loss coefficient also depends on the flow in the chamber. Figure 8(a) shows that loss coefficient decreases by 13% to 23% as the chamber length increases from 0.5*D* to 2.25*D*. This is due to pressure recovery associated with reattaching flow inside or at the lip of the chamber. Flow in the long-cavity mode has the largest pressure recovery and the lowest loss coefficient.

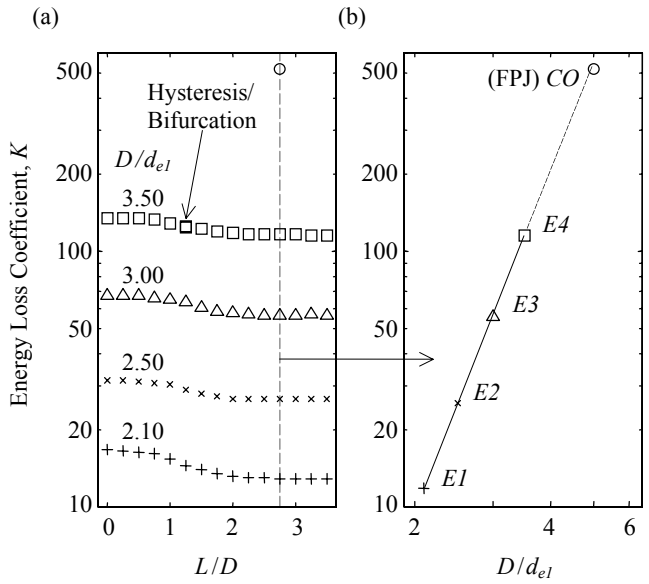

Figure 8. Variation in energy loss coefficient, K. +, ×, Δ, □, triangular orifice; ○, circular orifice:

(a) As a function of L/D at $\mathrm{Re}_1 = 50{,}000$.

(b) As a function of expansion ratio at $L/D = 2.75$ and with effects of varying Reynolds number averaged over $3{,}800 < \mathrm{Re}_1 < 60{,}400$.

For the largest expansion ratio there is a small step change in the loss coefficient at $L/D = 1.25$, which is the transition point between axisymmetric and asymmetric jet flow. This bi-stable flow is evidence of hysteresis or mathematical bifurcation. Once the oscillating jet flow is established, variations in L/D between 2.25 and 3.5 produce no further change in loss coefficient.

For fixed expansion ratio, the loss coefficient provides no indication of the amplitude of jet oscillation. In Figure 8(b), the loss coefficient is plotted on log-log axes as a function of the expansion ratio. All of the data fall on the curve:

$$K = 0.467(D/d_{e1})^{4.366}. \qquad (2)$$

An exponent of "4" rather than 4.366 would imply a constant discharge coefficient.

Conclusions

A nozzle consisting of a cylindrical chamber, a triangular inlet orifice and an outlet lip can produce a continuously oscillating jet with a large spreading angle. Except for the shape of the inlet orifice, this nozzle has a broadly similar geometry to the FPJ nozzle. Jet oscillation is produced with orifice expansion ratios ($2.1 \le D/d_{e1} \le 3.5$) much less than required for the FPJ nozzle. Therefore, the oscillating triangular jet can operate with a lower energy loss coefficient. In comparison with the FPJ, the triangular orifice produces continuous oscillation over a wider range of L/D ratios. The maximum jet-spreading angle occurs in the range $2.0 < L/D < 2.5$. The observed spreading angles are smaller than those produced by the FPJ. Investigations over a broader parameter range will reveal the maximum possible spreading angle.

The oscillating jet geometry which produces the maximum initial spreading angle coincides closely with the geometry which maximises the velocity decay rate. Maximum spreading angle and maximum decay rate increase with the expansion ratio of the orifice, and so there is a trade-off between pressure loss and decay rate.

The azimuthal direction of the oscillating jet is not uniformly distributed. Rather, the external jet oscillates rapidly between preferred locations corresponding to reattachment downstream from the straight sides of the orifice. Reattachment tends not to occur downstream from the corners of the orifice.

Acknowledgements

A SPIRT grant from the Australian Research Council and Fuel & Combustion Technology Pty. Ltd. is gratefully acknowledged.

References

[1] Davis, M. R., Variable Control of Jet Decay, *AIAA Journal*, Vol. **20**, No. 5, 1982, 606-609.

[2] Manias, C., Balendra, A. & Retallack D., New Combustion Technology for Lime Production, *World Cement*, December 1996.

[3] Mi, J., Nathan, G. J. & Luxton, R. E., Mixing Characteristics of a Flapping Jet from a Self-Exciting Nozzle, *Flow*, *Turbulence and Combustion*, (to appear in 2001).

[4] Mi, J., Nathan, G. J., Luxton, R. E. & Luminis Pty. Ltd., Naturally Oscillating Jet Devices, *Patent Application*, No. PP0421/97, 19 November 1997, PCT Application Filed, Australian Patent Office, 1998.

[5] Nathan, G. J., The Enhanced Mixing Burner, *Ph.D. Thesis*, Department of Mechanical Engineering, Adelaide University, Adelaide, Australia, 1988.

[6] Nathan, G. J., Hill, S. J. & Luxton, R. E., An Axisymmetric "Fluidic" Nozzle to Generate Jet Precession, *J. Fluid Mech*., Vol. **370**, 1998, 347-380.

[7] Quinn, W. R., Mean Flow and Turbulent Measurements in a Triangular Turbulent Free Jet, *Int. J. Heat and Fluid Flow*, Vol. **11**, No. 3, 1990, 220-224.

[8] Raman, G. & Cornelius, D. M., Jet Mixing Control Using Excitation from Miniature Oscillating Jets, *AIAA Journal*, Vol. **33**, No. 2, 1994, 365-368.

[9] Raman, G. & Rice, E. J., Axisymmetric Jet Forced by Fundamental and Subharmonic Tones, *AIAA Journal*, Vol. **29**, No. 7, 1991, 1114-1122.

[10] Raman, G., Rice, E. J. & Cornelius, D. M., Evaluation of Flip-Flop Jet Nozzles for Use as Practical Excitation Devices, *Transactions of the ASME*, *J. Fluids Eng.*, Vol. **116**, 1994, 508-515.

[11] Rapson, D., Stokes, B. & Hill, S. J., Kiln Flame Shape Optimization using a Gyro-Therm Gas Burner, *World Cement*, July 1995.

[12] Schadow, K. C., Gutmark, E., Parr, D. M. & Wilson, K. J., Selective Control of Flow Coherence in Triangular Jets, *Experiments in Fluids*, Vol. **6**, 1988, 129-135.

[13] Schadow, K. C., Gutmark, E. J., Wilson, K. J. & Smith, R. A., Noncircular Inlet Duct Cross-Section to Reduce Combustion Instabilities, *Combust. Sci. and Tech*., Vol. **73**, 1990, 537-553.

[14] Schneider, G. M., Structures and Turbulence Characteristics in a Precessing Jet Flow, *Ph.D. Thesis*, Department of Mechanical Engineering, Adelaide University, Adelaide, Australia, 1996.

[15] Simmons, J. M., Lai, J. C. S. & Platzer, M. F., Jet Excitation by an Oscillating Vane, *AIAA Journal*, Vol. **19**, No. 6, 1981, 673-676.

[16] Viets, H., Flip-Flop Jet Nozzle, *AIAA Journal*, Vol. **13**, No. 10, 1975, 1375-1379.